Journal of Biomechanics 176 (2024) 112327

Contents lists available at ScienceDirect

Journal of Biomechanics

journal homepage: www.elsevier.com/locate/jbiomech

Walking in a controlled ankle motion (CAM) boot: In-boot measurement of joint kinematics and kinetics

Mason L. Stolycia [a], David E. Lunn [a,b], Richard A. Wilkins [c,d], Cleveland T. Barnett [e], Josh Walker [a,*]

[a] Carnegie School of Sport, Leeds Beckett University, Leeds, United Kingdom
[b] NIHR Leeds Biomedical Research Centre, Leeds Teaching Hospitals NHS Trust, Leeds, United Kingdom
[c] Leeds Institute of Rheumatic and Musculoskeletal Medicine, University of Leeds, Leeds, United Kingdom
[d] Podiatry Department, Leeds Teaching Hospitals NHS Trust, Leeds, United Kingdom
[e] School of Science and Technology, Nottingham Trent University, Nottingham, United Kingdom

ARTICLE INFO

Keywords:
Foot and ankle orthoses
Achilles tendon
Rehabilitation
Gait
Orthotic device
Kinematic marker placement

ABSTRACT

Research investigating ankle function during walking in a controlled ankle motion (CAM) boot has either placed markers on the outside of the boot or made major alterations to the structure of the CAM boot to uncover key landmarks. The aim of this study was to quantify joint kinematics and kinetics using "in-boot" skin markers whilst making only minimal structural alterations. Seventeen healthy participants walked at their preferred walking speed in two conditions: (1) in standard athletic trainers (ASICS patriot 8, ASICS Oceania Pty Ltd, USA), and (2) using a hard-cased CAM boot (Rebound® Air Walker, Össur, Iceland) fitted on the right foot. Kinematic measurements revealed that CAM boots restrict sagittal plane ankle range of motion to less than 5°, and to ~3° in the frontal plane, which is a reduction of 85% and 73% compared to standard footwear, respectively ($p < 0.001$). This ankle restriction resulted in a reduction of ankle joint total limb work contribution from 38 ± 5% in normal footwear to 13 ± 4% in the CAM boot ($p < 0.001$). This study suggests that CAM boots do restrict the ankle joint's ability to effectively perform work during walking, which leads to compensatory mechanisms at the ipsilateral and contralateral hip and knee joints. Our findings align with previous research that employed "on-boot" kinematic measurements, so we conclude that in-boot approaches do not offer any benefit to the researcher and instead, on-boot measurements are suitable.

1. Introduction

Controlled ankle motion (CAM) boots are below-the-knee orthotic devices, encapsulating the foot and ankle, and sometimes the shank in the case of tall CAM boot models. They are regularly prescribed for ankle and foot pathologies (McHenry et al., 2017; Ready et al., 2018), including Achilles tendon rupture (Baxter et al., 2022), metatarsal fracture (Gonzalez et al., 2021), and foot ulceration resulting from diabetes mellitus (Bruening et al., 2022). The primary aim of CAM boots is to restrict or control the motion of the ankle joint and offload the foot whilst allowing a patient to continue ambulation throughout the healing or rehabilitation process (Ready et al., 2018).

Restricting or controlling ankle range of motion (RoM) could hinder the force-producing capacity of the muscles crossing the ankle joint (Böhm and Hösl, 2010). The reduction in RoM is ideal in the early phases of rehabilitation for its protective and restrictive purposes. However, with a limited ability to produce ankle work, there could be an increased demand on the knee and hip joints to compensate (Walker et al., 2024). Alterations to the kinetics and kinematics of these joints have been reported (Gulgin et al., 2018; Walker et al., 2024), suggesting an increased relative joint contribution of both ipsilateral and contralateral hip and knee joints, which might explain some secondary-site pain following CAM boot wear (Ready et al., 2018). These compensatory mechanisms might be caused by the increased effective mass or leg length of the CAM boot-wearing limb, or because of the assumed restriction in ankle motion.

When investigating the ankle joint's RoM during gait while wearing a CAM boot, previous research (Gulgin et al., 2018; Nahm et al., 2019; Sommer et al., 2022; Walker et al., 2024) has placed retroreflective markers on the external surface of the CAM boot. This approach assumes

* Corresponding author at: Carnegie School of Sport, Leeds Beckett University, Headingley Campus, Leeds LS6 3QT, United Kingdom.
E-mail address: josh.walker@leedsbeckett.ac.uk (J. Walker).

https://doi.org/10.1016/j.jbiomech.2024.112327
Accepted 12 September 2024
Available online 16 September 2024

that the underlying anatomical landmark did not move during gait trials. It also assumes that if there is no change in angle between the "foot" and "shank" segment orientations, this is reflecting no angle change inside the CAM boot. This assumption would result in the mechanical work done by the ankle inside the boot being zero. On the contrary, research has placed markers on anatomical structures in the boot via holes cut into CAM boots, attempting to quantify "in-boot" kinematics and kinetics (Zhang et al., 2006). This approach has resulted in opposing findings regarding ankle joint function, including no restriction in sagittal-plane ankle RoM, and higher ankle plantarflexion and inversion joint moments (Zhang et al., 2006). However, this approach requires careful consideration to avoid compromising the structural integrity of the CAM boots to maintain external and ecological validity. This is possible in hard-cased boots, but perhaps not in the soft-cased boots used by Zhang et al. (2006). As such, there is a need for a more robust approach to quantifying in-boot function during walking in CAM boots (Stolycia et al., 2024). This is especially important when calculating the ankle joint's mechanical work, and then exploring compensatory mechanisms at the ipsilateral hip and knee joints.

Previous literature explored strategically located cut-outs on conventional shoes to obtain underlying joint kinematics using in-shoe marker "clusters" (Alcantara et al., 2018; Shultz and Jenkyn, 2012), although these approaches have not been attempted in CAM boots. Therefore, the aim of this study was to quantify in-boot joint kinematics and kinetics during walking in a hard-cased CAM boot. This allowed us to directly quantify the magnitude of RoM restriction imposed on the ankle joint and any subsequent adaptation in joint kinematics and kinetics.

2. Methods

2.1. Participants

A convenience sample of 17 healthy individuals participated in this study (11 males, 6 females, age: 22 ± 2 years, height: 1.72 ± 0.68 m, body mass: 77.1 ± 13.9 kg). Participants completed medical screening prior to data collection and were confirmed free of any lower limb musculoskeletal injuries or conditions that might affect gait for the last 12 months. Participants also provided signed informed consent prior to data collection. Ethical approval was granted by the University's Local Research Ethics Committee and all data collection was conducted in accordance with the Declaration of Helsinki (World Medical Association, 2013).

2.2. Data collection procedures

Participants walked in two footwear conditions in a randomised order (randomised using two unmarked envelopes, which the participant blindly selected): (1) wearing a CAM boot (Rebound® Air Walker, Össur, Iceland) on the right leg (BOOT); and (2) wearing standardised athletic trainers (ASICS patriot 8, ASICS Oceania Pty Ltd, USA) bilaterally (SHOD). In BOOT, participants wore standardised trainers (ASICS patriot 8) on the left foot. CAM boot sizes included small, medium, and large, which were fitted to each participant's shoe size as per manufacturer guidelines. The standardised trainers were fitted to each participant's shoe size. In each footwear condition, participants walked overground over a flat surface at their preferred walking speed (PWS). External ground reaction forces (GRFs) were collected using three in-parallel 900- × 600-mm piezoelectric force platforms (9287B, Kistler, Germany) at 1000 Hz. Joint and segment kinematics were collected using a 14-camera optoelectronic motion capture system (Oqus 7+, Qualisys, Sweden) at 100 Hz. Participants were allowed several minutes to familiarise to both footwear conditions, before they walked repeatedly, with brief rest periods, along a 10-metre walkway. The force platforms and motion capture volume were located halfway along the walkway, as were two photocell timing gates (WittyGATE, Microgate, Italy), which were placed 2-m apart to measure, but not strictly control, PWS. Participants continued walking until five successful force platform contacts were obtained for both the ipsilateral (right) and contralateral (left) limbs.

Anatomical landmarks used for motion capture marker placement followed the calibrated anatomical systems technique (CAST) (Cappozzo et al., 1995), including: left and right anterior superior iliac spine, posterior superior iliac spine, greater trochanter, medial and lateral epicondyle of the femur, medial and lateral malleolus, calcaneus, and first, second, and fifth metatarsal heads, with 4-marker rigid clusters being placed on the lateral aspect of both thigh and shank segments. The markers used for the medial and lateral malleolus, as well as the first and fifth metatarsal heads and calcaneus, were custom 3D-printed "wand complexes" comprising of four non-coplanar markers (Fig. 1A, B) (Wilkins, 2021). These markers allowed us to locate anatomical landmarks whilst participants wore the CAM boot (Fig. 1C-E). To gain access to these landmarks, minor modifications were made to the CAM boot, with 29-mm (diameter) cut-outs made in relevant locations. The diameter was chosen to allow natural and uncompromised movement of the marker wands (Bishop et al., 2015) without impacting the structural integrity of the boots. This approach was also adopted on the right foot in the SHOD condition to ensure valid comparisons, with 17 × 25 mm oval cut-outs at relevant locations (Shultz and Jenkyn, 2012). It should be noted that the inflatable bladders which form part of the inlay of the CAM boots were compromised in this process; to account for this, foam infills were placed below participants' medial and lateral gastrocnemius muscle bellies to ensure that the boot was still restrictive around the shank.

2.3. Data processing

Marker trajectories were tracked and labelled in Qualisys Track Manager (version 2022.2, Qualisys, Sweden). In the event of marker dropout, polynomial interpolation was used to fill gaps shorter than 10 frames, and clusters were gap-filled using the rigid-body gap fill method where necessary. The markers on the wand complexes were all a known distance apart and a known distance from the base. This allowed for the position of the base to be triangulated as long as at least three of four markers were visible, thus allowing the position of the anatomical landmarks of the foot to be tracked. Marker trajectories and GRFs were exported to Visual3D (version 2023.08.3, C-Motion Inc., Canada) for skeletal modelling, where a seven-segment (pelvis [CODA], left thigh, right thigh, left shank, right shank, left foot, and right foot) 3D model was created from the static trials and applied to each movement trial (Wilkins, 2021).

Gait events for each ground contact (heel strike and toe-off) were determined using a 20-N vertical GRF threshold. Kinematic data (i.e., joint angles) were normalised to a percentage of the gait cycle (heel strike to ipsilateral heel strike). Joint kinetics were analysed during the stance phase (heel strike to toe-off). Joint mechanical work done was calculated in all three directions to obtain total mechanical work done by each joint. The sum of hip, knee, and ankle work done was then used to indicate the total mechanical work (TMW) for each limb. The relative contribution of each joint was calculated by calculating joint work as a percentage of TMW (Walker et al., 2024). All data were averaged across the five successful trials and exported to MATLAB (R2023a, MathWorks Inc., USA), where joint-level minima and maxima were computed for kinetics and kinematics, as well as subsequent variables of interest (e.g., RoM).

2.4. Statistical analysis

Statistical analyses were conducted using the Statistical Package for the Social Sciences (SPSS; version 28, IMB Inc., USA) and MATLAB. Paired student *t*-tests were used to compare discrete data between BOOT and SHOD conditions for each leg in isolation. Additionally, Cohen's

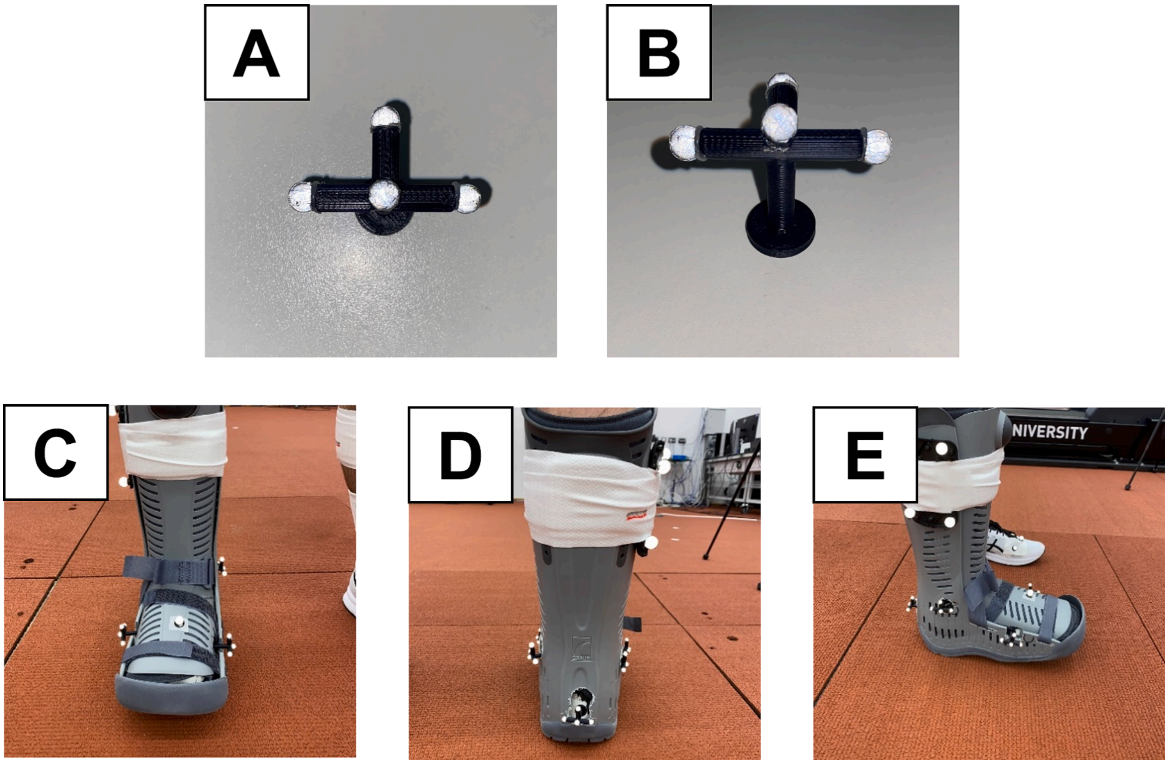

Fig. 1. Custom 3D-printed wand complexes placed on foot and ankle key anatomical landmarks in the current study (A and B). Anterior (C), posterior (D), and lateral (E) view of CAM boot marker set, including wand complexes.

d effect sizes were calculated and interpreted according to Hopkins et al. (2009): < 0.10 = "trivial"; 0.10–0.29 = "small"; 0.30–0.49 = "moderate"; 0.50–0.69 = "large"; 0.70–0.89 = "very large"; and ≥ 0.90 = "extremely large". As well as discrete statistical analysis, statistical parametric mapping (SPM) (Pataky, 2010) was carried out using 'spm1d' (version M.0.4.10) in MATLAB for paired student *t*-tests ('ttest_paired') for ankle joint angles. For all tests, significance level was set at $p < 0.05$.

3. Results

Ipsilateral peak ankle plantarflexion and dorsiflexion angles were both reduced in BOOT ($p < 0.001$) (Table 1). Contralateral peak dorsiflexion angle was also restricted in BOOT ($p = 0.002$), but peak plantarflexion was not ($p = 0.099$) (Table 1). As such, sagittal-plane ankle RoM was lower in BOOT ($p < 0.001$) for the ipsilateral limb, but not the contralateral ($p = 0.202$) (Table 1). Frontal-plane ankle kinematics were also different between BOOT and SHOD, with peak eversion ($p = 0.010$), inversion ($p < 0.001$), and RoM ($p < 0.001$) all being lower in BOOT (Table 1). There were no effects of condition on contralateral frontal-plane kinematics ($p \geq 0.086$) (Table 1).

Time-series analyses showed significant differences between BOOT and SHOD for sagittal-plane angles during early stance (~1–23% of the gait cycle), late stance (~36–55% of the gait cycle), and swing (~58–78% of the gait cycle) (Fig. 2). Similarly, in the frontal plane, ankle angle was different between BOOT and SHOD in the early (~6–38%) and late (~74–90%) phases of the gait cycle (Fig. 2).

Ipsilateral peak plantarflexion ($p < 0.001$) and dorsiflexion ($p = 0.016$) moments were both lower in BOOT (Table 2). Frontal-plane ankle moments were different between conditions in the ipsilateral limb, with peak eversion moment being significantly higher in BOOT ($p = 0.003$), although peak inversion moment was not different between conditions ($p = 0.501$) (Table 2). Contralateral ankle moments were similar between conditions (Table 2). Minimum and maximum sagittal-

Table 1
Discrete ankle joint kinematics for both limbs during SHOD and BOOT conditions.

Variable	Limb	SHOD	BOOT	t_{16}	*p-value*	Cohen's *d*
Peak dorsiflexion (°)	Contralateral	18.4 ± 3.1	17.1 ± 3.0	−3.61	0.002^{**}	0.88^{VL}
	Ipsilateral	17.8 ± 3.4	11.3 ± 2.5	−8.28	$<0.001^{***}$	2.01^{EL}
Peak plantarflexion (°)	Contralateral	−11.3 ± 6.6	−12.1 ± 7.1	−1.75	0.099	0.43^{M}
	Ipsilateral	−10.6 ± 5.7	7.0 ± 3.0	17.72	$<0.001^{***}$	4.30^{EL}
Sagittal RoM (°)	Contralateral	29.7 ± 5.0	29.2 ± 5.4	−1.330	0.202	0.32^{M}
	Ipsilateral	28.4 ± 4.3	4.3 ± 1.8	−26.84	$<0.001^{***}$	6.53^{EL}
Peak inversion (°)	Contralateral	2.8 ± 1.7	2.4 ± 1.8	−1.04	0.313	0.25^{S}
	Ipsilateral	8.4 ± 4.1	5.0 ± 2.6	−2.91	0.010*	0.71^{VL}
Peak eversion (°)	Contralateral	−5.9 ± 2.0	−6.4 ± 2.0	−1.83	0.086	0.44^{M}
	Ipsilateral	−3.1 ± 2.4	1.9 ± 2.5	7.21	$<0.001^{***}$	1.75^{EL}
Frontal RoM (°)	Contralateral	8.7 ± 1.7	8.8 ± 1.6	0.73	0.474	0.18^{S}
	Ipsilateral	11.5 ± 3.6	3.1 ± 0.9	−10.11	$<0.001^{***}$	2.45^{EL}

Note: The ipsilateral (right) limb was always the CAM boot-wearing limb. *, **, and *** denote significant differences at the $p < 0.05$, $p < 0.01$, and $p < 0.001$ level, respectively. For Cohen's *d* effect sizes, ^{T}=trivial, ^{S}=small, ^{M}=moderate, ^{VL}=very large, and ^{EL}=extremely large. No inter-limb comparisons were conducted. A negative kinematic value implies plantarflexion or eversion beyond "neutral" (Wu et al., 2002).

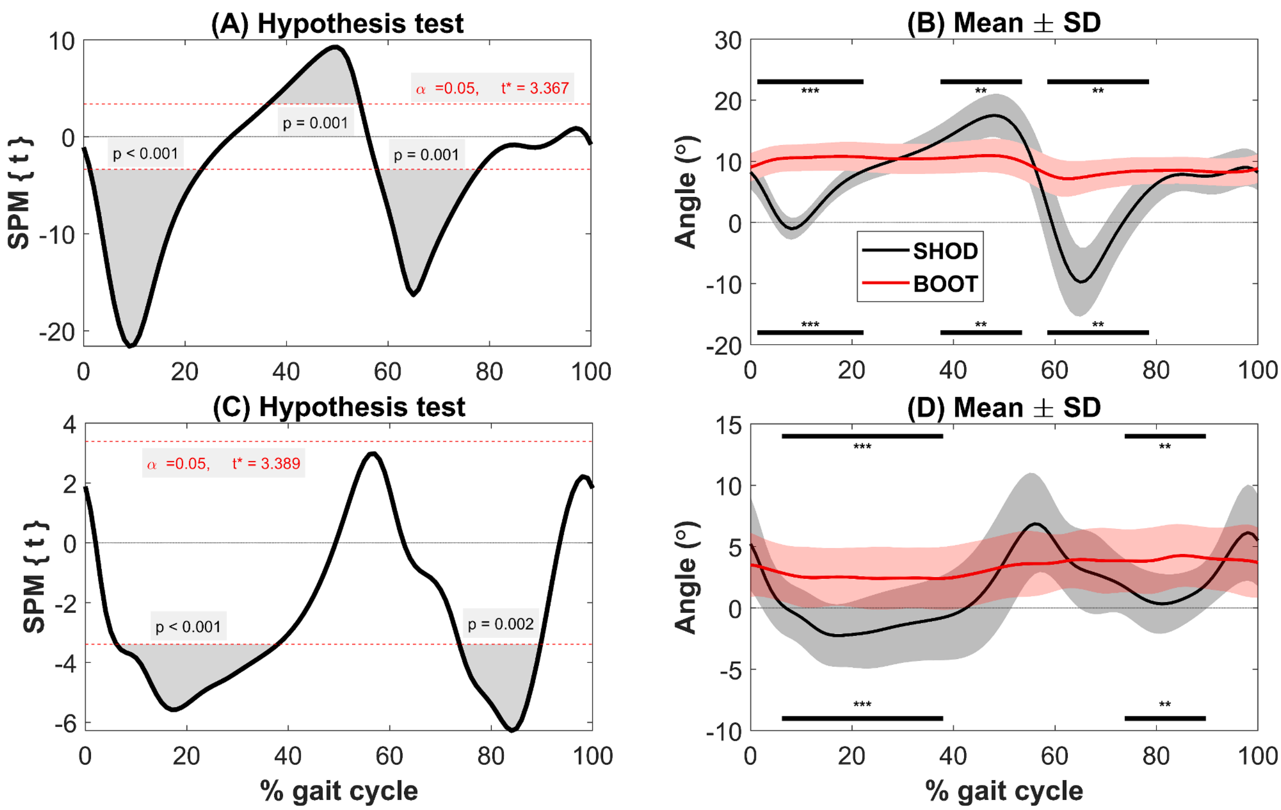

Fig. 2. Time-series comparisons of SHOD (black) and BOOT (red) ankle joint angles in the sagittal (A and B) and frontal (C and D) planes. In A and C, grey shaded areas denote suprathreshold clusters of significant differences, which are reflected in B and D with horizontal bars. ** and *** denote significant differences at the $p < 0.01$ and $p < 0.001$ level, respectively. (For interpretation of the references to colour in this figure legend, the reader is referred to the web version of this article.)

Table 2
Discrete ankle joint kinetics for both limbs during SHOD and BOOT conditions during the stance phase of the gait cycle.

Variable	Limb	SHOD	BOOT	t_{16}	*p-value*	Cohen's *d*
Peak DF moment (N•m/kg)	Contralateral	1.54 ± 0.20	1.49 ± 0.21	−1.28	0.218	0.31^{M}
	Ipsilateral	1.57 ± 0.22	1.71 ± 0.28	2.69	0.016*	0.65^{L}
Peak PF moment (N•m/kg)	Contralateral	−0.24 ± 0.08	−0.24 ± 0.05	0.32	0.754	0.08^{T}
	Ipsilateral	−0.25 ± 0.08	−0.08 ± 0.06	9.88	$<0.001^{***}$	2.40^{EL}
Minimum sagittal power (W/kg)	Contralateral	−1.04 ± 0.29	−0.81 ± 0.23	5.13	$<0.001^{***}$	0.77^{VL}
	Ipsilateral	−0.97 ± 0.31	−0.16 ± 0.10	12.10	$<0.001^{***}$	2.93^{EL}
Maximum sagittal power (W/kg)	Contralateral	3.25 ± 0.87	2.94 ± 0.84	−2.43	0.027*	0.59^{L}
	Ipsilateral	3.30 ± 0.90	0.71 ± 0.36	−12.96	<0.001	3.14^{EL}
Peak inversion moment (N•m/kg)	Contralateral	−0.08 ± 0.06	−0.10 ± 0.08	−1.24	0.235	0.30^{M}
	Ipsilateral	−0.12 ± 0.09	−0.13 ± 0.12	−0.688	0.501	0.17^{S}
Peak eversion (N•m/kg)	Contralateral	0.14 ± 0.07	0.15 ± 0.09	0.77	0.454	0.19^{S}
	Ipsilateral	0.09 ± 0.07	0.03 ± 0.06	−3.52	0.003^{**}	0.85^{VL}
Minimum frontal power (W/kg)	Contralateral	−0.18 ± 0.08	−0.17 ± 0.09	0.63	0.540	0.15^{S}
	Ipsilateral	−0.24 ± 0.07	−0.05 ± 0.03	10.42	$<0.001^{***}$	2.53^{EL}
Maximum frontal power (W/kg)	Contralateral	0.04 ± 0.03	0.06 ± 0.04	3.19	0.006^{**}	0.74^{VL}
	Ipsilateral	0.09 ± 0.06	0.04 ± 0.02	−2.90	0.010*	0.70^{VL}

Note: PF = plantarflexion, DF=dorsiflexion. The ipsilateral (right) limb was always the CAM boot-wearing limb. *, **, and *** denote significant differences at the $p < 0.05$, $p < 0.01$, and $p < 0.001$ level, respectively. For Cohen's *d* effect sizes, ^{T}=trivial, ^{S}=small, ^{M}=moderate, ^{L}=large, ^{VL}=very large, and ^{EL}=extremely large. No inter-limb comparisons were conducted.

plane ankle power were lower in BOOT for both ipsilateral ($p < 0.001$) and contralateral ($p \leq 0.027$) limbs (Table 2). Ipsilateral minimum and maximum frontal-plane ankle power was also reduced in BOOT ($p \leq 0.010$), whereas the contralateral limb had lower maximum frontal-plane ankle power in SHOD ($p = 0.006$) (Table 2).

Ipsilateral TMW was lower in BOOT (0.84 ± 0.14 J/kg) compared with SHOD (1.40 ± 0.22 J/kg) ($t_{16} = -11.96$, $p < 0.001$, $d = 2.90$ [extremely large]; Fig. 3B). This was accompanied by less hip work (BOOT = 0.39 ± 0.07 J/kg vs. SHOD = 0.48 ± 0.07 J/kg, $t_{16} = -7.67$, $p < 0.001$, $d = 1.86$ [extremely large]) and ankle work (BOOT = 0.11 ± 0.04 J/kg vs. SHOD = 0.53 ± 0.11 J/kg, $t_{16} = -16.47$, $p < 0.001$, $d = 3.99$ [extremely large]) in BOOT compared with SHOD (Fig. 3B). However, knee work was not significantly different between BOOT (0.35 ± 0.07 J/kg) and SHOD (0.38 ± 0.10 J/kg) ($t_{16} = -1.93$, $p = 0.071$, $d = 0.47$ [moderate]; Fig. 3B). TMW in the contralateral limb was lower in BOOT (1.29 ± 0.23 J/kg) compared with SHOD (1.40 ± 0.21 J/kg) ($t_{16} = -3.99$, $p = 0.001$, $d = 0.97$ [extremely large]; Fig. 3A). This was accompanied by less knee work (BOOT = 0.33 ± 0.10 J/kg vs. SHOD = 0.39 ± 0.12 J/kg, $t_{16} = -5.04$, $p < 0.001$, $d = 1.22$ [extremely large]) and ankle work (BOOT = 0.49 ± 0.09 J/kg vs. SHOD = 0.53 ± 0.10 J/

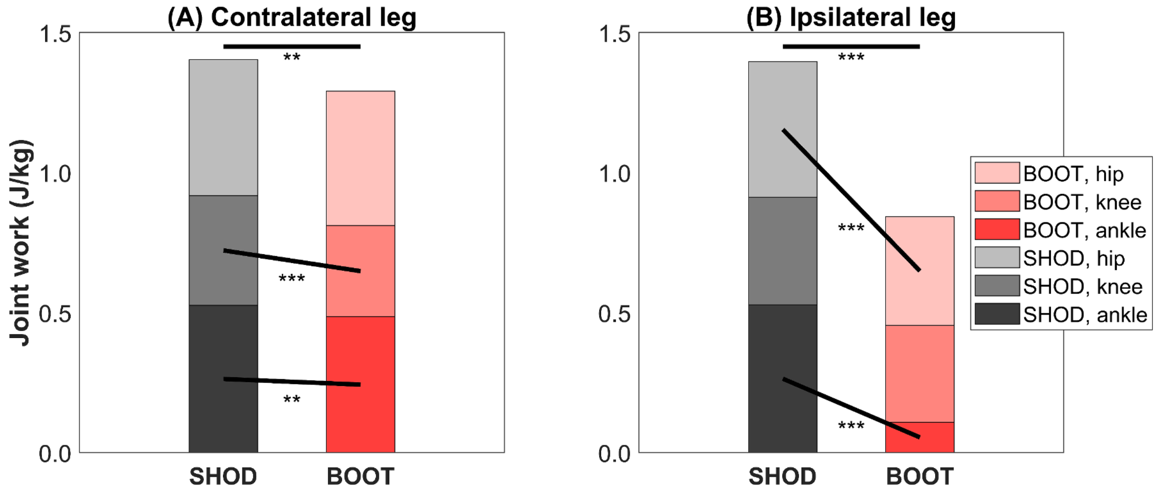

Fig. 3. Joint mechanical work done by the hip, knee, and ankle for the contralateral (left) leg (A) and ipsilateral (right) leg (B) during walking in the SHOD (black) and BOOT (red) conditions. The sum of all three joints equates to TMW. Significant differences are represented by black bars connecting SHOD and BOOT comparisons. ** and *** denote significant differences at the $p < 0.01$ and $p < 0.001$ level, respectively. (For interpretation of the references to colour in this figure legend, the reader is referred to the web version of this article.)

kg, $t_{16} = -2.94$, $p = 0.010$, $d = 0.71$ [very large]) in BOOT compared with SHOD (Fig. 3A). However, hip work was similar between BOOT (0.49 ± 0.06 J/kg) and SHOD (0.48 ± 0.08 J/kg) ($t_{16} = -0.33$, $p = 0.747$, $d = 0.08$ [trivial]; Fig. 3A).

The ipsilateral hip joint's contribution to TMW was higher in BOOT (46 ± 5%) than SHOD (35 ± 4%) ($t_{16} = 11.56$, $p < 0.001$, $d = 2.80$ [extremely large]; Fig. 4B). The knee joint's contribution to TMW was also higher in BOOT (41 ± 4%) than SHOD (27 ± 5%) ($t_{16} = 17.63$, $p < 0.001$, $d = 4.28$ [extremely large]; Fig. 4B), whereas the ankle joint's contribution was lower (BOOT: 13 ± 4% vs. SHOD: 38 ± 5%; $t_{16} = -20.74$, $p < 0.001$, $d = 5.03$ [extremely large]; Fig. 4B). In the contralateral limb, the hip joint's contribution to TMW was higher in BOOT (37 ± 4%) than SHOD (35 ± 3%) ($t_{16} = 4.52$, $p < 0.001$, $d = 1.10$ [extremely large]; Fig. 4A). However, the knee joint's contribution was lower (BOOT: 25 ± 4% vs. SHOD: 28 ± 5%; $t_{16} = -4.14$, $p = 0.001$, $d = 1.00$ [extremely large]; Fig. 4A). There was no difference between BOOT (38 ± 5%) and SHOD (38 ± 5%) for the ankle's contribution to TMW ($t_{16} = -0.17$, $p = 0.866$, $d = 0.04$ [trivial]; Fig. 4A).

Preferred walking speed was lower in BOOT (1.29 ± 0.18 m/s) than SHOD (1.37 ± 0.18 m/s) ($t_{16} = -5.12$, $p < 0.001$, $d = 1.24$ [extremely large]).

4. Discussion

The aim of this study was to quantify in-boot ankle joint kinematics and kinetics during walking in a hard-cased CAM boot. This was achieved using a novel marker-based approach to minimise structural alterations to the boot. In-boot ankle joint RoM was limited to less than 5° in the sagittal plane, and ∼ 3° in the frontal plane. This equates to ∼ 85% and ∼ 73% reductions when comparing to walking in normal footwear, respectively. The restricted RoM led to compensatory responses at more proximal ipsilateral joints and in the contralateral limb, which was characterised by an increase in ipsilateral knee and hip joint work contribution, as well as altered hip and knee contributions in the contralateral leg.

In the current study, ankle RoM was restricted in both the sagittal and frontal planes, showing that the CAM boot is an effective orthotic device for use in pathological populations as an alternative to plaster casts. Time-series analyses showed this was particularly evident in early stance when BOOT restricted plantarflexion, and then at late stance/

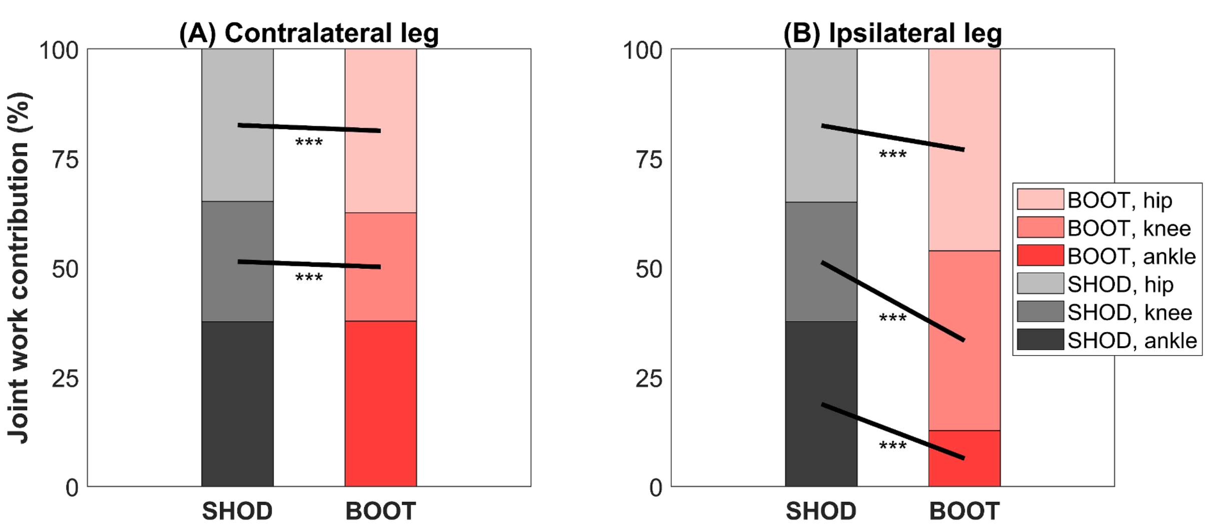

Fig. 4. Relative joint contribution to TMW by the hip, knee, and ankle for the contralateral (left) leg (A) and ipsilateral (right) leg (B) during walking in the SHOD (black) and BOOT (red) conditions. Significant differences are represented by black bars connecting SHOD and BOOT comparisons. *** denotes significant differences at the $p < 0.001$ level. (For interpretation of the references to colour in this figure legend, the reader is referred to the web version of this article.)

early swing when BOOT limited the ankle joint's ability to rapidly switch from dorsiflexion to plantarflexion (Fig. 2B), which is a common mechanism in normal walking associated with elastic energy return from the Achilles tendon. As such, these findings suggest that the CAM boot used the current study was able to protect the Achilles tendon from unwanted strain, which could be beneficial for early-stage rehabilitation. It was able to quantify this with minimal compromise to the structural integrity of the CAM boot by using smaller holes than previous research (see Fig. 1 in Zhang et al., 2006), whilst the design of the markers (Fig. 1) allowed the tracking of key anatomical landmarks throughout the entire gait cycle. Ankle joint RoM being less than 5° in BOOT was expectedly lower than in SHOD (Table 1; Fig. 2). This low RoM aligns with studies using on-boot markers for kinematic measurements during walking in CAM boots (Gulgin et al., 2018; Nahm et al., 2019; Sommer et al., 2022; Walker et al., 2024). The findings of this study also align with studies that used videofluoroscopy to observe in-boot kinematics (McHenry et al., 2017; Nahm et al., 2019). Videofluoroscopy is often impractical because of the limited capture volume which can influence gait patterns, and radiation exposure can limit the number of trials that can be collected. As such, our novel approach allows valid and feasible kinematic information to be collected whilst ensuring the participants' gait was unaffected.

The reductions in joint RoM during BOOT predictably led to significant reductions in ankle power (Table 2), which in-turn, reduced ankle joint mechanical work (Fig. 3). Ipsilateral ankle work was reduced by ~ 80% in BOOT (0.11 ± 0.04 J/kg vs. 0.53 ± 0.22 J/kg in SHOD), proving that the ankle capacity to do work (with regards to both energy absorption and generation) during walking in a CAM boot is diminished. This is beneficial in the early stages of rehabilitation following injuries to the Achilles tendon. However, it should be noted here that ankle work done was not fully eliminated by CAM boot wear. This does align with some previous research that used the on-boot kinematic approach (Walker et al., 2024). Given this appears to be the case whether an in-boot or on-boot approach is adopted, the ankle work measured could be caused by deformation of the CAM boots during stance, or measurement error. Although not directly comparable because of methodological differences (treadmill versus overground walking, PWS differences, etc.), the ankle work presented by Walker et al. (2024) is approximately half of that presented in the current study (Fig. 3). This was also reflected in the ankle joint's relative contribution to TMW, which was also substantially lower in BOOT than SHOD (Fig. 4).

The current study also proved that the relative contribution of ipsilateral hip and knee joints increases in BOOT to compensate for the restriction at the ankle joint (Fig. 4). These compensatory mechanisms reflect those presented using on-boot kinematics (Walker et al., 2024), and likely explain some of the secondary-site pain commonly reported following CAM boot wear (Ready et al., 2018). Similarly, alterations in the contralateral limb were also found, including the hip and knee joints' relative contributions to TMW. The hip joint contributed more to TMW, whilst the knee joint contributed less (Fig. 4), which we hypothesise could be caused by the leg length discrepancy caused by CAM boot wear. These impacts can be partially mitigated by the administration of an "even-up" walker or "shoe leveller" (Bruening et al., 2022; Walker et al., 2024), although these are not always provided as standard care. Nonetheless, researchers and clinicians who are investigating CAM boot function and patient management using CAM boots should consider the impact on other lower-limb joints, including those on the contralateral, non-CAM boot-wearing limb.

Results from the current study should be interpreted in light of its limitations. Firstly, PWS was lower in BOOT compared to SHOD, which led to a reduction in TMW for both the ipsilateral and contralateral limbs. This partially explains our choice to present relative joint contributions to TMW alongside joint work, although it does make direct comparisons more difficult. Nonetheless, allowing participants to walk at PWS is more ecologically valid than controlling gait speed and more representative of a "true" acute response to CAM boot wear. PWS was also not controlled between trials for each participant to maintain ecological validity. However, within-subject, inter-trial variation was low (coefficient of variation < 10%) and was similar between BOOT (4 ± 2%) and SHOD (3 ± 1%) across participants. It should be considered that the population that was recruited were all healthy participants with no lower extremity injuries which would affect their natural gait. This allowed us to understand the mechanisms of the CAM boot, isolating its impact on gait without considering the biomechanical effects of injury. However, this does have implications for ecological validity and transferability into a clinical setting. Patients with pathologies such as Achilles injury, where CAM boots are often prescribed to aid rehabilitation, might have different mechanical responses and compensatory mechanisms during CAM boot use. Finally, having a minimal effect on the structural integrity of the boot was considered greatly when cutting holes to allow access to the anatomical landmarks of the foot and ankle. Although it can be assumed that the size of the holes did not have a detrimental effect on the structural integrity of the CAM boots used, we did not conduct any material testing to confirm this. The inflatable bladder which sits between the shank and the casing of the boot was also punctured. To overcome this, foam padding was used mimic the effects of the bladder, create a tight fit by filling in any potential spaces within the boot.

5. Conclusions

The use of a CAM boot is an effective method for restricting ankle joint RoM to less than 5° in the sagittal plane, and ~ 3° in the frontal plane during walking. This limited the ankle joint's ability to contribute to the overall mechanical work done by the CAM boot-wearing limb to 13%, compared to 38% in normal footwear. This change was compensated for by increases in the contribution of the ipsilateral hip and knee joints. Our results align with previous on-boot kinematic measurements, and not in-boot measurement where substantial modifications to the boot have been made. As such, it seems that there are no benefits to attempting in-boot kinematics unless using videofluoroscopy, so on-boot measurements are recommended for future research. However, future research should look to systematically explore the optimal marker placement on CAM boots to improve fidelity of foot and ankle kinematics and kinetics, possibly by directly comparing in-boot and on-boot approaches or by including radiographic imaging.

Funding

This research did not receive any specific funding.

CRediT authorship contribution statement

Mason L. Stolycia: Writing – review & editing, Writing – original draft, Visualization, Validation, Software, Methodology, Investigation, Formal analysis, Data curation, Conceptualization. **David E. Lunn:** Writing – review & editing, Writing – original draft, Supervision, Methodology, Conceptualization. **Richard A. Wilkins:** Writing – review & editing, Writing – original draft, Supervision, Methodology, Conceptualization. **Cleveland T. Barnett:** Writing – review & editing, Writing – original draft. **Josh Walker:** Writing – review & editing, Writing – original draft, Visualization, Supervision, Software, Project administration, Methodology, Investigation, Formal analysis, Conceptualization.

Declaration of competing interest

The authors declare that they have no known competing financial interests or personal relationships that could have appeared to influence the work reported in this paper.

References

Alcantara, R.S., Trudeau, M.B., Rohr, E.S., 2018. Calcaneus range of motion underestimated by markers on running shoe heel. Gait Posture 63, 68–72.

Baxter, J.R., Hullfish, T.J., Farber, D.C., Humbyrd, C.J., 2022. Achilles Tendon Loading During Walking Differs Between Commonly Used Immobilizing Boots. Foot & Ankle Orthopaedics 7, 2473011421S2473000576.

Bishop, C., Arnold, J.B., Fraysse, F., Thewlis, D., 2015. A method to investigate the effect of shoe-hole size on surface marker movement when describing in-shoe joint kinematics using a multi-segment foot model. Gait Posture 41, 295–299.

Böhm, H., Hösl, M., 2010. Effect of boot shaft stiffness on stability joint energy and muscular co-contraction during walking on uneven surface. J. Biomech. 43, 2467–2472.

Bruening, D.A., Huber, S.C., Parry, D.J., Hillier, A.R., Hayward, A.E.M., Grover, J.K., 2022. The effect of existing and novel walker boot designs on offloading and gait mechanics. Med. Eng. Phys. 108, 103890.

Cappozzo, A., Catani, F., Della Croce, U., Leardini, A., 1995. Position and orientation in space of bones during movement: anatomical frame definition and determination. Clin. Biomech. 10, 171–178.

Gonzalez, L.J., Johnson, J.R., Konda, S.R., Egol, K.A., 2021. The fifth metatarsal shaft fracture is well treated with benign neglect. Foot Ankle Spec.

Gulgin, H., Hall, K., Luzadre, A., Kayfish, E., 2018. 3D gait analysis with and without an orthopedic walking boot. Gait Posture 59, 76–82.

Hopkins, W.G., Marshall, S.W., Batterham, A.M., Hanin, J., 2009. Progressive statistics for studies in sports medicine and exercise science. Med. Sci. Sports Exerc. 41, 3–12.

McHenry, B.D., Exten, E.L., Cross, J.A., Kruger, K.M., Law, B., Fritz, J.M., Harris, G., 2017. Sagittal subtalar and talocrural joint assessment during ambulation with controlled ankle movement (CAM) Boots. Foot Ankle Int. 38, 1260–1266.

Nahm, N., Bey, M.J., Liu, S., Guthrie, S.T., 2019. Ankle motion and offloading in short leg cast and low and high fracture boots. Foot Ankle Int. 40, 1416–1423.

Pataky, T.C., 2010. Generalized n-dimensional biomechanical field analysis using statistical parametric mapping. J. Biomech. 43, 1976–1982.

Ready, L.V., Fisk, E.G., Ciurylo, W., Chiodo, C.P., Bluman, E.M., Smith, J.T., 2018. Associated joint pain with controlled ankle movement walker boot wear. JAAOS Global Res. Rev. 2.

Shultz, R., Jenkyn, T., 2012. Determining the maximum diameter for holes in the shoe without compromising shoe integrity when using a multi-segment foot model. Med. Eng. Phys. 34, 118–122.

Sommer, B., Hollenstein, A., Graf, E., 2022. Stability boots for the treatment of Achilles tendon injuries: gait analysis of healthy participants. Gait Posture 91, 131–136.

Stolycia, M.L., Lunn, D.E., Stanier, W., Walker, J., Wilkins, R.A., 2024. Biomechanical effectiveness of controlled ankle motion boots: a systematic review and narrative synthesis. J. Foot Ankle Res. 17, e12044.

Walker, J., Thomas, A., Stolycia, M.L., Wilkins, R.A., Lunn, D.E., 2024. Acute biomechanical responses to wearing a controlled ankle motion (CAM) walker boot during walking. Gait Posture 108, 208–214.

Wilkins, R.A., 2021. Haemarthrosis of the ankle in haemophilia A and B: prevalence, impact and intervention. University of Leeds. PhD Thesis.

World Medical Association, 2013. World medical association declaration of helsinki. ethical principles for medical research involving human subjects. J. Am. Med. Assoc. 310, 2191–2194.

Zhang, S., Clowers, K.G., Powell, D., 2006. Ground reaction force and 3D biomechanical characteristics of walking in short-leg walkers. Gait Posture 24, 487–492.